Supporting Information

Stabilizing LAGP/Li interface and in-situ visualizing the interfacial structure evolution for high-performance solid-state lithium metal batteries

Jin Li [a], Junjie Chen [a], Xiaosa Xu [a], Jing Sun* [a], Baoling Huang* [a], Tianshou Zhao* [a,b]

[a] Department of Mechanical and Aerospace Engineering, The Hong Kong University of Science and Technology, Clear Water Bay, Kowloon, Hong Kong SAR, China
[b] Department of Mechanical and Energy Engineering, Southern University of Science and Technology, Shenzhen, 518055, China

E-mail: jsunav@connect.ust.hk (J. Sun); mebhuang@ust.hk (B.L. Huang); zhaots@sustech.edu.cn (T.S. Zhao).

Experimental Procedures

Materials and chemicals:

DOL monomer, (1,3-dioxolane) and LAGP ($Li_{1.5}Al_{0.5}Ge_{1.5}(PO_4)_3$) and LLZTO ($Li_{6.4}La_3Zr_{1.4}Ta_{0.6}O_{12}$) powder, solvent DEC and FEC (Diethyl carbonate and fluoroethylene carbonate), LiTFSI (Lithium bis(triffuoromethanesulfonyl)imide), $EMImNTF_2$ (1-Ethyl-3-methylimidazolium bis(trifluoromethylsulfonyl)imide) and $LiPF_6$ (Lithium hexafluorophosphate) was provided by SuZhou Fosai New Material Co., Ltd. Super P powder, polyvinylidene fluoride (PVDF, MW = 1,000,000), $LiCoO_2$ and $LiFePO_4$ were purchased from Shenzhen Kejing Star Tech Co. Ltd. NMP (N-methylpyrrolidone) , GF (glass fiber) were provided by Aladdin and used as received. All above chemicals are obtained commercially and used without any further purification.

Material synthesis:

The QCPE@P-DOL films were prepared by in situ polymerization technique. Usually, the nano-LAGP powder, monomers DOL, LiTFSI, $EMImNTF_2$, and $LiPF_6$ were added to solvent (DEC/FEC = 7: 3 (v / v)), and the mixture was stirred vigorously to form a homogeneous solution. The order of addition is: dissolve $LiPF_6$ in solvent, dissolve LiTFSI into DOL and stir to obtain a homogeneous solution. Then, $EMImNTF_2$ and LAGP were added into the DOL solution, stirred evenly, and mixed with all liquid to obtain the precursor solution after stirring. Finally, the mixture is quickly injected into the assembled 2032-coin cell until the glass fiber (GF) is fully permeated. The cells were then kept at room temperature for 24 hours to ensure that DOL and $LiPF_6$ were fully polymerized. Due to the selective adsorption of GF and ring-opening polymerization of DOL, LAGP@P-DOL accumulates on one side of GF membrane and P-DOL electrolyte fills GF. Using the same method, replacing LAGP with LLZTO, electrolyte QCPE1@P-DOL was obtained.

The preparation of electrolyte QCPE uses the same material as above, and the specific operation steps are as follows: $LiPF_6$, LiTFSI and $EMImNTF_2$ are added into solvent and stir to obtain a homogeneous solution. Then, LAGP are added into DOL and stirred evenly. Finally, add solvent solution and DOL solutions into the assembled 2032-coin cell one after another until the glass fiber (GF) is fully permeated. The cells were then kept at room temperature for 24 hours to ensure that DOL and $LiPF_6$ were fully polymerized. Due to the selective adsorption of GF and ring-opening polymerization of DOL, LAGP accumulates on one side of GF membrane and P-DOL

electrolyte fills GF. Using the same method, replacing LAGP with LLZTO, electrolyte QCPE1 was obtained.

The electrolyte compositions and corresponding values are provided in Table S1. The conductivity is optimized by adjusting the ratio of DOL and solvent to select the most suitable electrolyte. Five kinds of precursors, (X wt% (DOL) (X=30, 40, 50, 60 and 70) + (100-X) wt% solvent)) were allowed to be cured at RT to form three-dimensional cross-linked network QCPEs for a sake of comparison. They are referred to as Q_{30}CPE-5, Q_{40}CPE-5, Q_{50}CPE-5, Q_{60}CPE-5 and Q_{70}CPE-5, respectively. According to the polymerization state and conductivity of the electrolyte, the most suitable electrolyte is selected as Q_{60}CPE-5. The concentration of LAGP in QCPEs was 2.5, 5, 7.5 and 10 wt% of the total mass (DOL + Solvent), referred to as Q_{60}CPE-2.5, Q_{60}CPE-5, Q_{60}CPE-7.5 and Q_{60}CPE-10. Among them, the highest conductivity is Q_{60}CPE-5, namely QCPE@P-DOL.

Electrode preparation and battery assembly:

For the preparation of cathodes, the slurries were prepared by mixing active materials ($LiFePO_4$ and $LiCoO_2$) with super P and polyvinylidene difluoride (PVDF) binder (mass ratio = 8:1:1) in N-methyl-2-pyrrolidone (NMP). The obtained slurries were casted on the carbon coated Al foils and then dried in vacuum oven for 24 h at 80 °C. The foil was punched into discs (diameter 12 mm) used as cathode, and Li metal foils (450 μm) were used as anode. The areal loading of dried LFP and $LiCoO_2$ were a range from 2 mg cm^{-2} to 3 mg cm^{-2}, The content of highly loaded cathode materials used in the manuscript has been explained. The solid–state lithium metal batteries were assembled by sandwiching the QCPEs between cathode and Li anode in CR2032 coin cells in Ar-filled glovebox (Mikrouna, H_2O, $O_2 \leq 0.1$ ppm).

Materials characterization:

The morphology and structure of the QCPEs were characterized by a scanning electron microscope (SEM) with an acceleration voltage of 5 kV, Fourier transform infrared (FT-IR) spectroscopic, and Transmission electron microscope (TEM). The symmetrical lithium batteries were disassembled in an argon-filled glove box. The lithium sheet can be tested for the surface morphology and chemical composition after treatment with DMC. The surface morphology and chemical composition of Li anode were analyzed by XPS, Time of Flight Secondary Ion Mass Spectrometry (TOF-SIMS) and SEM. The LFP|QCPE@P-DOL|Li batteries were disassembled in an argon-filled glove box. Cryo-TEM was used to observe the morphology and composition of the

interface at the atomic level. In-situ TEM techniques, combined with nanoscale battery configurations, offer valuable visual insights into the structural evolution and phase transitions of materials during cycling. In this study, a LAGP@P-DOL/LAGP sphere was attached to a gold wire as an electrode, while a tungsten wire with a piece of Li/Li_2O served as the counter electrode. By applying a negative bias to the tungsten wire, LAGP/LAGP@P-DOL underwent lithiation, followed by delithiation when the bias was reversed to a positive value.

Electrochemical measurements:

Assemble the battery in a glove box filled with argon. For electrochemical testing, the half-cell was charged and discharged at a constant current between 2.5V and 3.8V with LFP cathode (The theoretical discharge capacity is 170 mAh g^{-1}); the half-cell was charged and discharged at a constant current between 2.8V and 4.45V with $LiCoO_2$ cathode (The theoretical discharge capacity is 178 mAh g^{-1}) A charge-discharge cycle study was conducted on the battery test system (Xinwei, China). The ionic conductivity of solid-state electrolytes was tested by Biological at open circuit voltage in the frequency range of 100 kHz–0.1 Hz with amplitude 10 mV at temperatures from 25 °C to 70 °C. The measurement sample was prepared by sandwiching the electrolyte between two stainless steel disc electrodes, where the electrolyte film has a size of 18 mm. The ionic conductivity (σ) of electrolyte membranes was calculated according to the Equation:

$$\sigma = \frac{L}{R_b S}$$

R_b was the bulk resistance of the electrolytes obtained from AC impedance spectroscopy and L and S were the thickness (cm^2) and area (cm^2) of the solid electrolyte.

Activation energy (E_a) can be calculated according to the Arrhenius equation:

$$\sigma = AT^{-1}e^{\frac{-E_a}{RT}}$$

The value of prefactor A is related to the effective charge carrier concentration.

The lithium-ion transference number (t_{Li^+}) was tested by chronoamperometry combined with electrochemical impedance spectroscopy using a symmetric cell of Li/QCPEs/Li battery, and it can be calculated according to the equation below:

$$t_{Li^+} = \frac{I_S\,(\Delta V - I_0 R_0)}{I_0\,(\Delta V - I_S R_S)}$$

Where I_0 and I_s are the initial DC current and steady-state DC current respectively;

R_O and R_s are the initial and steady-state interface resistances; ΔV is the applied pulse potential of 10 mV.

the Li^+ diffusion coefficient was calculated based on the EIS measurements with LFP|QCPEs|Li cells according to the following equations:

$$D = \frac{R^2 T^2}{2A^2 n^2 F^2 C^2 \sigma^2}$$

$$Z_{real} = R_S + R_{CT} + \sigma\omega^{-0.5}$$

where R, F, and T were respectively ideal gas constant, Faraday constant, and the absolute temperature, A represented the area of the electrode, n was the number of electrons per molecule during oxidization and C was the concentration of Li^+, σ represented the Warburg factor that could be calculated from the relationship of Z' versus $\omega^{-0.5}$.

DFT and COMSOL calculations:

All the calculations are performed in the framework of the density functional theory with the projector augmented plane-wave method, as implemented in the Vienna ab initio simulation package[1]. The generalized gradient approximation proposed by Perdew-Burke-Ernzerhof (PBE) is selected for the exchange-correlation potential[2]. The cut-off energy for plane wave is set to 480 eV. The energy criterion is set to 10^{-5} eV in the iterative solution of the Kohn-Sham equation. All the structures are relaxed until the residual forces on the atoms have declined to less than 0.02 eV/Å. To avoid interlaminar interactions, a vacuum spacing of 20 Å is applied perpendicular to the slab. The most stable crystal structure of $Li_{1.5}Al_{0.5}Ge_{1.5}(PO_4)_3$ was doped with Al^{3+} in the form of $Li_{1+x}Al_xGe_{2-x}(PO_4)_3$ via the partial replacing of Ge^{4+}. And Li atoms were added at the nearest 36f position to maintain the neutrality of the material. Using LAGP as a model solid electrolyte, the Li/P-DOL, Li/LAGP and P-DOL/LAGP interface models were constructed. Then the lattice parameters and atomic positions from the constructed interface models have been relaxed to satisfy the convergence requirement, which could be evaluated by energy difference between an interface system and the separated slab energies of the two materials that comprised it.

The interfacial formation energy is expressed as:

$$E = \frac{E_i - \sum E_s}{A}$$

E_i denotes the total energy of the complete system containing the interface, E_s denotes the total energy of the separated slabs (Li, P-DOL, and LAGP), and A referees to the

interfacial area.

Considering that the dendrite formation process of the lithium ion deposition is related to electrode dynamics and ion migration caused by diffusion, the moving boundary of the lithium surface can be tracked using COMSOL Multiphysics 6.0, coupled with "cubic current distribution, Nernst Planck" interface and "deformation geometry". The ionic mobility was calculated by Nernst-Einstein relation, and the diffusion coefficient and conductivity were determined by the electrolyte. The electrode reaction was described by the Butler-Vollmer equation, and the deposition rate was determined by Faraday determination.

The basic model is as follows:

Conservation of current $\nabla \cdot i_s = Q_s$;

Ohm's law $i_s = -\sigma_s \nabla \emptyset_s$;

Where i_s denotes the current density vector of the electrode (A/m^2), σ_s denotes the conductivity (S/m), ∂_s denotes the electrode potential (V), Q_s denotes the general current source term (A/m^3).

Net electrolyte current density $i_l = F \sum_i z_i N_i$;

Electrolyte ion flux $N_i = -D_i \nabla c_i - z_i u_{m,i} F c_i \nabla \emptyset_l + c_i u$;

Electrolyte current conservation $\nabla \cdot i_l = Q_l$;

Matter conservation $\frac{\partial \varepsilon_l c_i}{\partial t} + \nabla \cdot N_i = R_i$;

i_l denotes the current density vector of the electrolyte (A/m^2), F denotes the Faraday constant (C/mol), N_i denotes the flux of i (mol/(m^2·s)), the charge number of the i is z_i, c_i denotes the concentration of ion i (mol/m^3), D_i denotes the diffusion coefficient (m^2/s), $u_{m,i}$ denotes the mobility (s·mol/kg), ∂_l denotes the electrolyte potential, u denotes the velocity vector (m/s), R_i is the electrochemical reaction rate.

The level set interface is used to track the deformation of the Anode surface during deposition. The interface is represented by the 0.5 contour of the level set variable. The level set variable Φ changes from 1 in the electrolyte domain to 0 in the deposition region, so the level set variable can be regarded as the electrolyte volume fraction.

The transport of the level set variable is given by:

$$\frac{\partial \Phi}{\partial t} + u \cdot \nabla \Phi = \gamma \nabla \cdot (\varepsilon \nabla \Phi - \Phi(1-\Phi)\frac{\nabla \Phi}{|\nabla \Phi|})$$

The level set delta function is approximated by:

$$\delta = 6|\Phi(1-\Phi)||\nabla \Phi|$$

The velocity field used in the transport equation for level set variable is evaluated from the

lithium deposition reaction current density:

$$u = n \cdot (-\frac{i_{loc}}{F}\frac{M_{Li}}{\rho_{Li}})$$

The interface normal n is calculated as:

$$n = \frac{\nabla \Phi}{|\nabla \Phi|}$$

The ε determines the thickness of the interface, defined as $\varepsilon = max/4$, where h_{max} is the maximum mesh size in the domain. γ determines the number of reinitializations, i_{loc} is the local current density, M_{Li} is the molar mass, and ρ_{Li} is the density of lithium.

The change of local current density with potential and lithium concentration is described by Bulter-Volmer equation.

$$i_{loc} = i_0(\exp\left(\frac{1.5F\eta}{RT}\right) - \frac{c_{Li^+}}{c_{Li^+,ref}}\exp\left(-\frac{0.5F\eta}{RT}\right)$$

The rate of electrochemical reaction is:

$$R_i = -\frac{v_i i_v}{nF}$$

Cathode surface:

$$N_{Li^+} \cdot n = -\frac{i_{loc}}{F}$$

Other boundary insulation, electrolyte anion insulation conditions are applied to all boundaries.

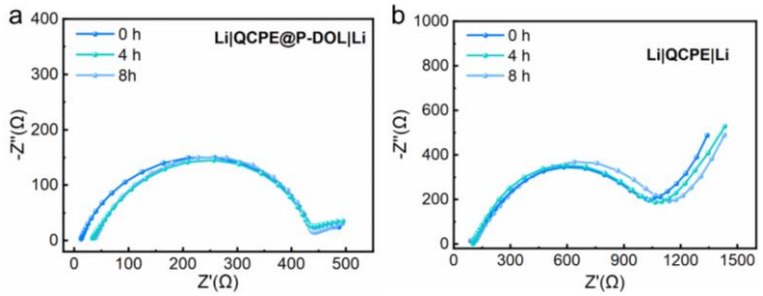

Fig. S1. EIS measurements of the Li/CPEs/Li cells at different resting times with (a) QCPE@P-DOL and (b) QCPE.

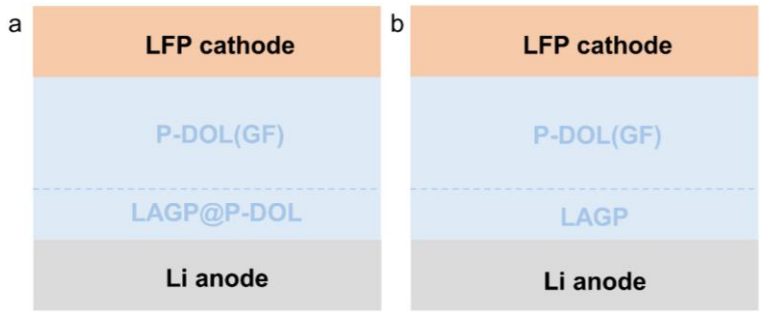

Fig. S2. Schematic setup of the LFP||Li cell with (a) QCPE@P-DOL and (b) QCPE

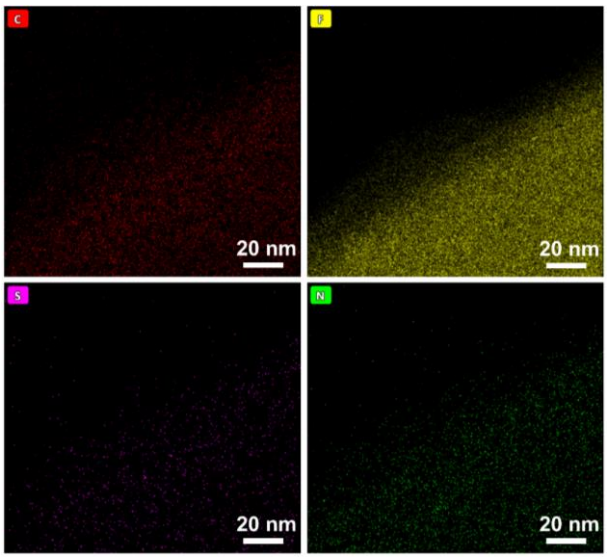

Fig. S3. The corresponding distributions of C, F, S and N elements.

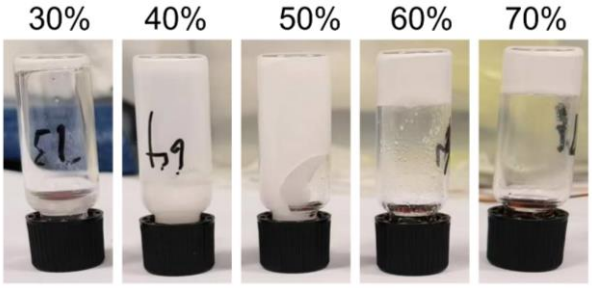

Fig. S4. Optical photos after polymerization of precursor solution with different mass contents of DOL (the total amount is DOL and solvent).

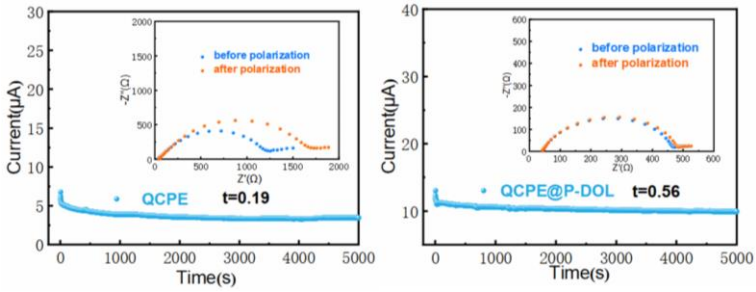

Fig. S5. Polarization curve with a 10 mV DC voltage of QCPE and QCPE@P-DOL at 25 ℃. (Insets are AC impedance spectra before and after polarization).

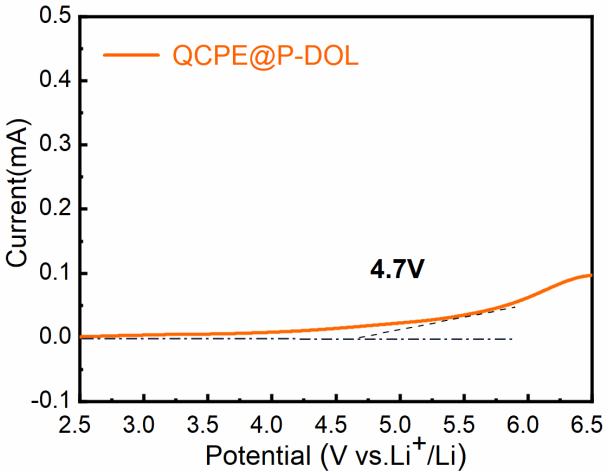

Fig. S6. Electrochemical stability windows with QCPE@P-DOL.

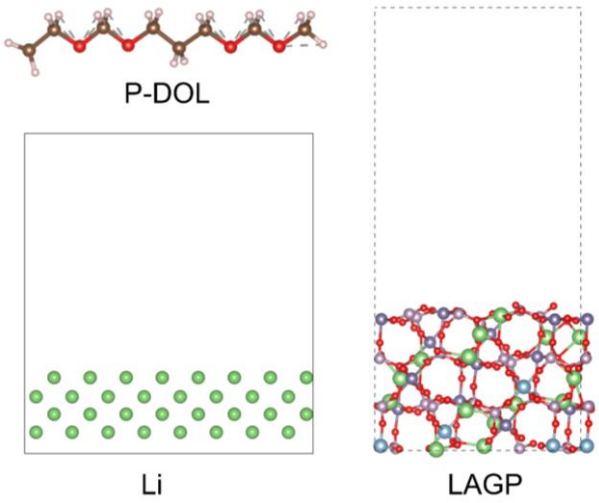

Fig. S7. the molecular models of P-DOL, Li, and LAGP. Color code: Li (green), C (brown), O (red), H (white), P (light purple), Ge (purple), Al (blue).

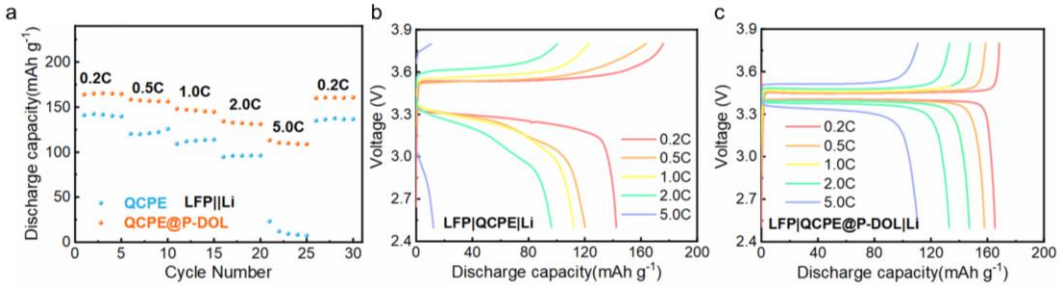

Fig. S8. (a) C-rate performances at various rates from 0.2 C to 5.0 C at 30 ℃. The corresponding charge and discharge voltage profiles under different rates (c) QCPE. (d) QCPE@P-DOL.

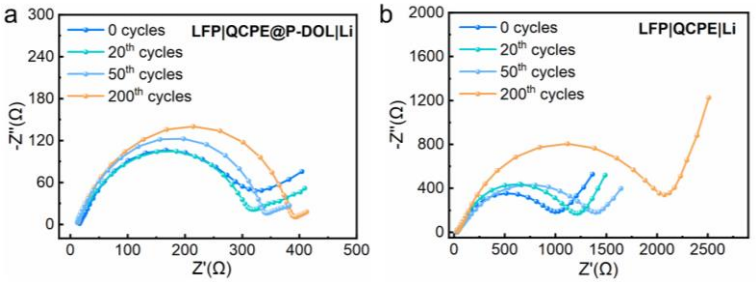

Fig. S9. EIS measurements of the LFP/CPEs/Li cells at different cycles with (a) QCPE@P-DOL and (b) QCPE.

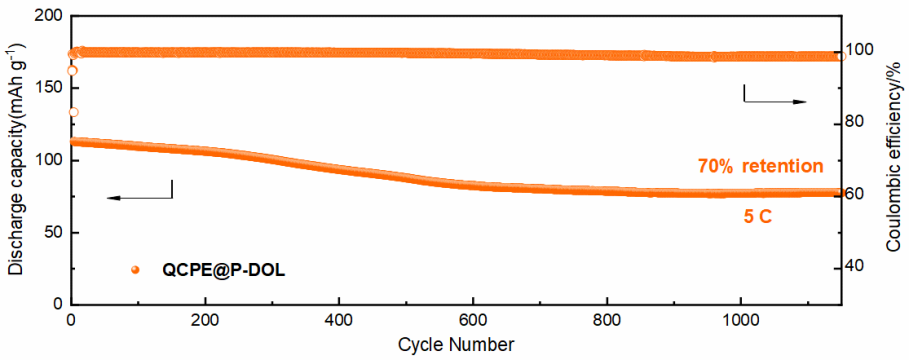

Fig. S10. Long cycling performances of $LiFePO_4$ batteries with QCPE@P-DOL under 5.0 C at 30 ℃.

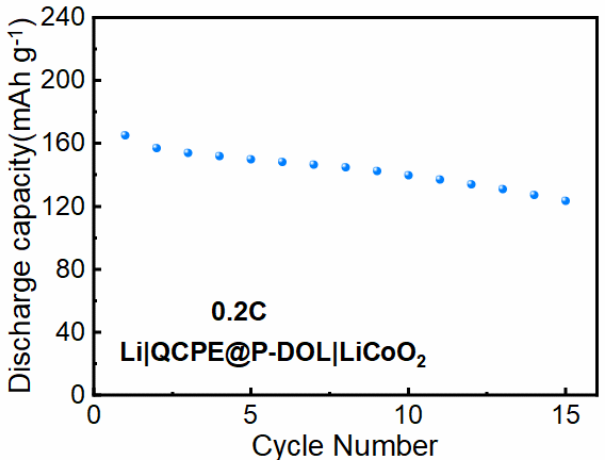

Fig. S11. Cycling performances of $LiCoO_2$ batteries with QCPE@P-DOL under 0.2 C at 30 ℃.

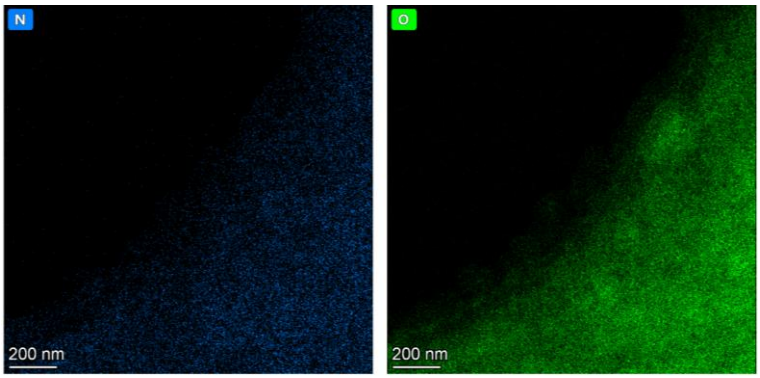

Fig. S12. The corresponding distributions of N and O elements.

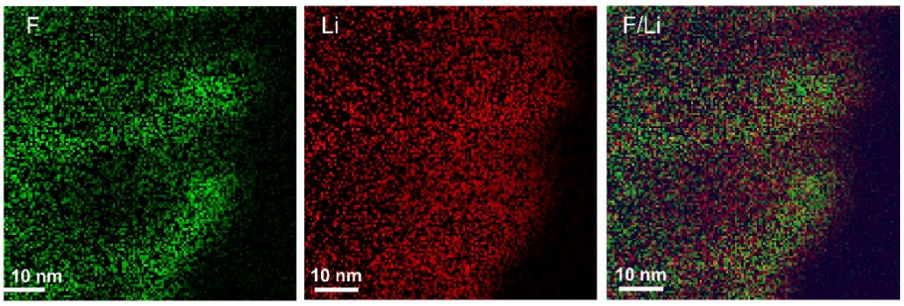

Fig. S13. EELS elemental mapping of F and Li.

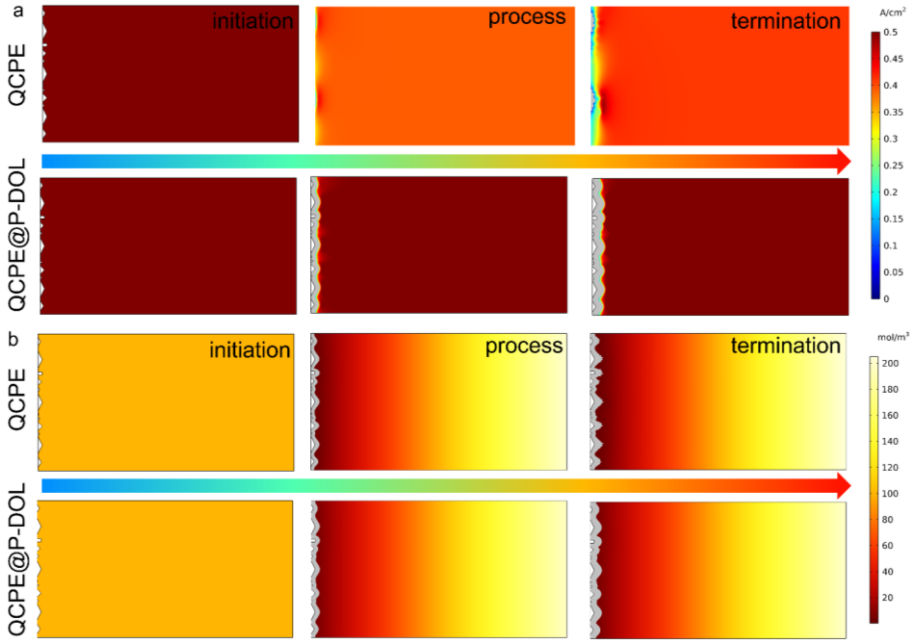

Fig. S14. (a-b) Current density and surface concentration simulation distributions at time of QCPE and QCPE@P-DOL.

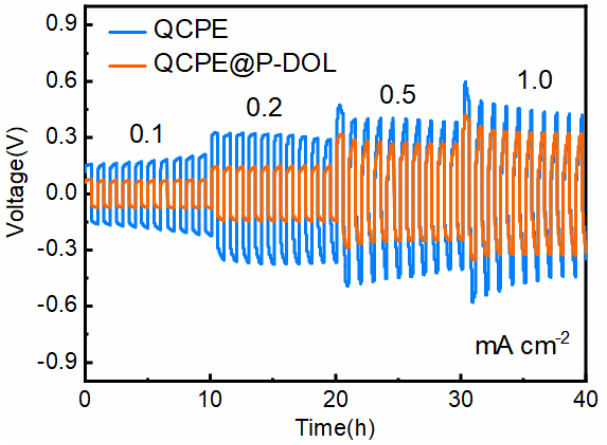

Fig. S15. Lithium symmetric battery test with different CPEs at various current densities ranging from 0.1 to 1.0 mA cm^{-2}.

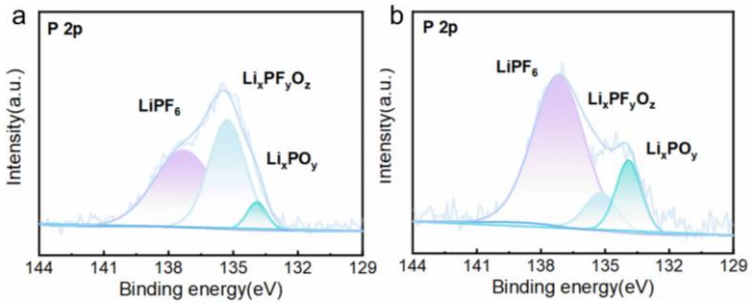

Fig. S16. (a-b) XPS spectra of cycled Li discs with P 2p spectrum (a) QCPE (b) QCPE@P-DOL.

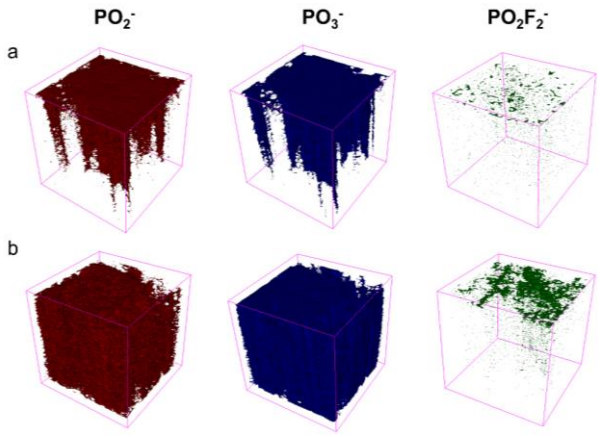

Fig. S17. Corresponding 3D reconstruction (PO_2^-, PO_3^-, and $PO_2F_2^-$) of Li anode with (a) QCPE@P-DOL and (b) QCPE.

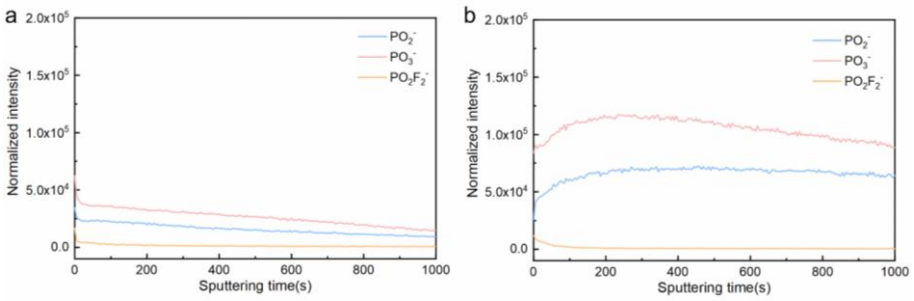

Fig. S18. TOF-SIMS negative ion depth profiles on the cycled Li electrode disassembled from (a) Li|QCPE@P-DOL|Li and (b) Li|QCPE |Li cells.

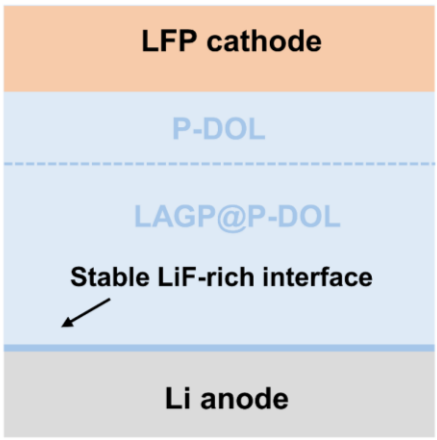

Fig. S19. Schematic setup of the LFP|QCPE@P-DOL|Li cell and LiF-rich interface.

Table S1. The compositions of electrolyte used to optimize ionic conductivity.

Electrolytes	DOL (mg)	Solvent (mg)	LiTFSI (mg)	$LiPF_6$ (mg)	EMIMTFSI (μL)	LAGP (mg)	RT Ionic conductivity (mS cm^{-1})
Q_{30}CPE-5	300	700	287	152	100	50	3.75
Q_{40}CPE-5	400	600	287	152	100	50	1.88
Q_{50}CPE-5	500	500	287	152	100	50	1.07
Q_{60}CPE-5	600	400	287	152	100	50	1.48
Q_{70}CPE-5	700	300	287	152	100	50	1.31
Q_{60}CPE-2.5	600	400	287	152	100	25	0.65
Q_{60}CPE-7.5	600	400	287	152	100	75	0.93
Q_{60}CPE-10	600	400	287	152	100	100	0.80
QCPE	600	400	287	152	100	50	0.96

Q_{60}CPE-5 is named QCPE@P-DOL

Table S2. The detailed data of the interfacial formation energies of the Li|P-DOL, LAGP|Li, and LAGP|P-DOL.

	E_total(eV)		E_slab(eV)	E_interface binding(eV)	A($Å^2$)	σ(eV/$Å^2$)	Surface Energy σ(J/m^2)
Li-(P-DOL)	-273.89	Li	-108.08	-1.56	156.01	-0.01	-0.16
		P-DOL	-164.24				
LAGP-Li	-1208.11	LAGP	-1095.33	-12.15	171.11	-0.07	-1.14
		Li	-100.63				
LAGP-(P-DOL)	-1262.74	LAGP	-1095.33	-3.16	171.11	-0.02	-0.30
		P-DOL	-164.24				

References

1. G. Kresse and D. Joubert, *Physical Review B*, 1999, **59**, 1758-1775.
2. J. P. Perdew, K. Burke and M. Ernzerhof, *Physical Review Letters*, 1996, **77**, 3865-3868.